THE CLEVELAND ELECTRIC ILLUMINATING COMPANY

P.O. BOX 5000 - CLEVELAND, OHIO 44101 - TELEPHONE (216) 622-9800 - ILLUMINATING BLDG. — 55 PUBLIC SQUARE

Serving The Best Location in the Nation

MURRAY R. EDELMAN
VICE PRESIDENT
NUCLEAR

July 11, 1984
PY-CEI/NRR-0123 L

Mr. B. J. Youngblood, Chief
Licensing Branch No. 1
Division of Licensing
U. S. Nuclear Regulatory Commission
Washington, DC 20555

Perry Nuclear Power Plant, Units 1 & 2
Docket Nos. 50-440; 50-441
SER Outstanding Issue No. 9
LOCA-Related Pool Dynamic Loads

Dear Mr. Youngblood:

This letter and attachment provide additional information to clarify four topics discussed in the May 2, 1984 meeting with the NRC staff and their consultants on LOCA-related pool dynamic loads (SER Outstanding Issue No. 9).

Attachment 1 to this letter describes the methodology for two Perry Nuclear Power Plant unique analysis and provides the evaluation of two generic items. The Perry specific analysis of the effects of gratings at the 599' elevation and the analysis of the bulk impact pressure on the steam tunnel are described, including the application of the SOLAV computer code. Additionally, the combined effects of increased submergence and encroachments on local loads, and the effect of encroachments on the SRV load definitions are discussed. These evaluations conclude that existing design load definitions bound the effects of these conditions.

We believe this additional information will resolve the staff concerns and enable SER Outstanding Issue No. 9 to be resolved in a future supplement to the SER.

Very truly yours,

P. Kaplan for M. Edelman

Murray R. Edelman
Vice President
Nuclear Group

MRE:njc

Attachments

cc: Jay Silberg, Esq.
John Stefano
J. Grobe

A001
1/1

1. 3B.10 - Loads on Structures Between the Pool Surface and the HCU Floors.

The method used to analyze the effect of gratings and structures at the 599' elevation is specified in Appendix 1. The calculations show that the two-dimensional SOLAV radial velocity distribution was used to obtain an average velocity squared term which was input into the one-dimensional pressure drop calculation.

As explained in Appendix 1, the best estimated clean pool velocity was 39 ft/sec while the best estimate maximum surface velocity when the 599' floor structures are taken into account, is 40 ft/sec. The FSAR clean pool velocity, on the other hand, reaches 46 ft/sec due to the substantially higher driving pressure.

The maximum local pool boundary pressure would be expected to occur in the vicinity of the largest radial encroachment. The boundary load is a function of both the bubble pressure and the distance from the bubble to the pool boundary (containment wall). The largest encroachment (9.5 feet for Perry) translates the bubble closest to the containment wall and causes the pressure to remain high. As demonstrated in the Perry-unique encroachment analysis, the expected boundary loads for this encroachment configuration remain less than the design loading (10 psid).

The methodology used to analyze the effect of grating at the 599' elevation is a global analysis. Three situations which exist at Perry have been qualitatively evaluated and for the following reasons are not considered a problem:

A.) Grating extends 3 feet from drywell wall.
Since this is such a small extension, a significant perturbation of the pool swell transient would not occur even if the grating was a solid encroachment.

B.) Grating extends across pool.
Since the grating extends completely across the pool, a relatively uniform loss will occur. In this situation, the global analysis performed is applicable.

C.) Grating extends 3 feet from encroachment.
This small extension is not expected to significantly effect the transient since: (1) the restriction is 6 feet above the pool, thus having no effect until the bubble pressure is substantially reduced late in the transient. (2) Since the grating has 70% open area with a depth of only 2 1/4", significant flow area still remains. (3) The extension is only 3 feet.

APPENDIX 1

Method of Analysis

In order to determine the effects on global response, the 599' floor has been assumed to be a uniformly distributed flow restriction above the entire suppression pool surface. The restrictions caused by the upper and lower flanges of the supporting I-beams and the floor grating have been lumped into two discrete losses occuring at 596' 6" and 599' 9". The loss at the lower elevation account for the restriction due to the bottom flanges of the supporting I-beams. The loss at the higher elevation accounts for the beam top flanges and the floor grating. The area of the pool taken up and encroachments was assumed to effectively cause a restriction in the pool free flow area since the amount of area affected is nearly constant in the vicinity of the 599' floor. Both the losses were modelled as orifices. The loss factors were determined using Reference 1. They are

$$K_{596'} = .25 \tag{1}$$

and

$$K_{599'} = .44 \tag{2}$$

These losses were then used with velocities output from the SOLAV computer code to find an average pressure drop due to the 599' floor. The following equation was used for this calculation.

$$\rho = 1/2 \quad K_{596} \quad (V^2_{596}) + 1/2 \quad K_{599} \quad (V^2_{599}) \tag{3}$$

An iterative procedure was used to converge on the expected drywell pressure including the effects of the 599' floor and the weir grating. The first step in the procedure was to use the containment analysis model, M3CPT04 (Reference 2), to determine the best estimate drywell and wetwell pressure histories for a main steamline break. This analysis included the effect of the weir grating by treating it as a uniform vent flow loss. The loss coefficient is $K_W = 1.4$ as opposed to $K_W = 1.0$ for no grating.

Best estimate calculations were done by modelling the break flow with the Homogeneous Equilibrium Model (HEM), and modelling other parameters associated with the break flow (such as quality) to match PSTF data, as described in Reference 3. These pressures were then input into a General Electric proprietary version of the SOLA-VOF fluid dynamics computer program (SOLAV) to determine the clean pool (without 599' floor modelled) response for a design basis pool swell transient. The resultant nodal velocities gave an upper bound for the pool swell velocity because the effect of the 599' floor is to slow down the rising water slug. The upper bound velocities gave an upper bound for the average pressure drop due to the 599' floor. The pressure drop was then added to the wetwell airspace pressure and again input into SOLAV. This run yielded a lower bound for the pool swell velocity and 599' floor pressure drop because it assumed the 599' floor slows the pool swell but doesn't increase the drywell pressure. The bubble pressure which SOLAV calculated for this run is an upper bound because bubble pressure is inversely related to pool swell velocity. Thus, the second iteration was begun by imposing the SOLAV upper bound of bubble pressure on the M3CPT code.

The drywell and wetwell pressure histories were generated and the SOLAV calculations were repeated using the established procedure.

Calculation of the second iteration 599' floor pressure drop showed that it had converged to the first iteration values. Thus, the feedback of pressure to the drywell does not significantly impact the pool swell calculations.

The second iteration SOLA run with the 599' floor pressure drop added to the wetwell pressure gives an upper bound for pressures in the suppression pool below the 599' floor. The boundary load history for the containment wall was taken from this run.

A modified model for SOLAV bubble pressure and wetwell pressure was necessary to determine the effects of the 599' floor on water slug velocity above the floor. This model required that the dynamics above the 599' be modelled correctly. In order to do this, the upper bound for bubble pressure was found from the SOLAV run that yielded the upper bounding pool boundary condition, the wetwell pressure history was modified. Prior to the time when the bubble passes through the 599' floor, the bubble expansion is restricted by the pressure drop due to the floor. After passage of the bubble through the floor it is able to expand, unrestricted by the floor. As before the pressure drop of the floor was added to the wetwell pressure before the bubble passed the 599' floor. After reaching the floor the additional pressure was no longer added to the wetwell pressure. Thus, the water slug was accelerated, unrestricted by the 599' floor, after passing through the floor. This anlaysis showed the maximum slug velocity reaches 40 ft/s. an increase of less than 3 percent from the clean pool best estimate slug velocity which is 39 ft/sec.

References

1. Idel'chik, "Handbook of Hydraulic Resistance", AEC-Tr-6630, 1960

2. Bilanin, W. J., "The General Electric Mark III Pressure Supression Containment Analytical Model", (NEDO)-20533, June, 1974."

3. GESSAR II, Appendix 3B, Attachment 0, Figure 3B.3-5, GE Doc. 22A7000, Rev.2, June 1981.

2. Steam Tunnel Load Definition

The Perry steam tunnel is designed in accordance with the NRC Draft Acceptance Criteria (Appendix C to the Draft Technical Evaluation Report on Mark III LOCA-Related Hydrodynamic Load Defination provided by memo dated 10/8/82 form Mr. Themis P. Speis (NRC) to Mr. Hank Pfefferlen (GE)). We have also evaluated the steam tunnel because of plant specific SOLAV predictions and have concluded the steam tunnel is adequately designed. The plant specific SOLAV methodology is as follows:

To determine the Perry steam tunnel loading, the first step was to define the total vertical pool momentum at the time when the pool surface first impacted the steam tunnel.

$$I_{total} = \sum_{\text{all cells}} Mi\ Vi = \sum_{\text{all cells}} Fi\ Wi\ di\ Li\ Vi \qquad (1)$$

where

Mi = mass in cell i
Vi = velocity in cell i
Fi = fluid fraction in cell i
di = cell i depth
Wi = cell i width
Li = cell i length
I total = total pool impulse (momentum)

To convert this to a per unit area basis, it is necessary to divide by the impacted area A, which is

$$a = m\ Widi$$

where m = # of cells in impacted area = 10

The duration of the impact is the time it takes for the total impacted length of the steam tunnel to be filled with water. No credit is taken for circumferential curvature or flow, minimizing the impact duration. This time was determined by first calculating the average surface velocity at the time of initial impact (11.4 ft/sec) and the average distance from the pool surface to the steam tunnel bottom surface (2.7 feet). Then the duration to fill the space under the steam tunnel neglecting circumferential flow is merely

$$= \frac{\text{Avg. distance traveled}}{\text{Avg. Velocity}} = \frac{2.7 \text{ ft.}}{11.4 \text{ ft/sec}} = 237 \text{ msec} \qquad (3)$$

This is shown more clearly in Figure 2.

Knowing the total impulse per unit area and impulse duration, the maximum impact pressure is specified once a waveform is determined. Using an isosceles triangle or versed sine as the loading shape, it may be shown that

$$P_{max} = 2\ (I/A)/ \qquad (4)$$

$$= 2\ (248 \text{ lbf sec/ft}^2)/.237 \text{ sec}/144 \text{ in}^2/\text{ft}^2$$

$$= 14.5 \text{ psi}$$

This maximum calculated pressure will be reduced by gravity since the momentum previously considered was the total amount at the initial impact. The gravity effect may be accounted for as

$$\frac{I}{A}_{gravity} = \frac{1}{2} P L_s = 96 \text{ lbf sec/ft}^2$$

where

L_s = average slug length = 13 ft.
= impulse duration = .237 sec.

When gravity is factored into the maximum pressure calculation, it is seen that the maximum impact pressure is only 8.9 psi. This calculated loading was increased to 15 psia for design application.

Modeling the steam tunnel directly with SOLAV would not provide a realistic representation of the actual impact loading because:

1. The wetwell airspace would pressurize since rising pool surface would trap air between the pool surface and the steam tunnel. This pressurization would increase the impact duration and is not modeled with SOLAV.

2. An impact loading is a local effect with duration specified through an accoustic relaxation time, the relatively large SOLAV mesh size and time steps will not resolve the actual loading.

An isosceles triangle was selected as the impact waveform since:

1. This is the same waveform as the design froth impact load. The similar waveforms will increase calculational simplicity.

2. Since the actual loading will occur as the rising pool sweeps across the underside of the tunnel, a flatter loading distribution would probably occur. Using the isosceles triangle provides a more peaked loading which increases the structural response (dynamic loading factor).

FIGURE 1 STEAM TUNNEL GEOMETRY

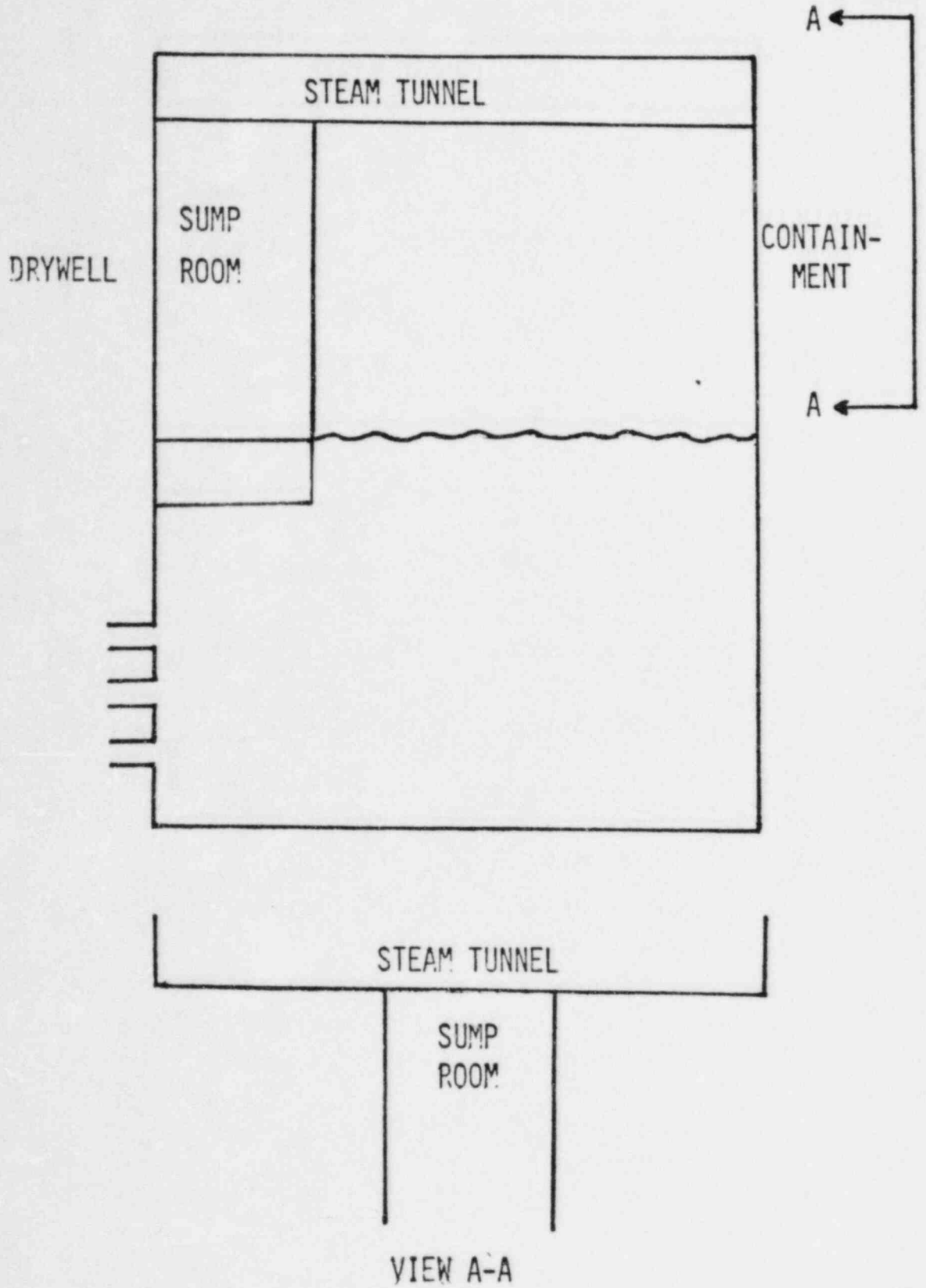

EJM
6/5/84

FIGURE 2 POOL CONFIGURATION AT IMPACT

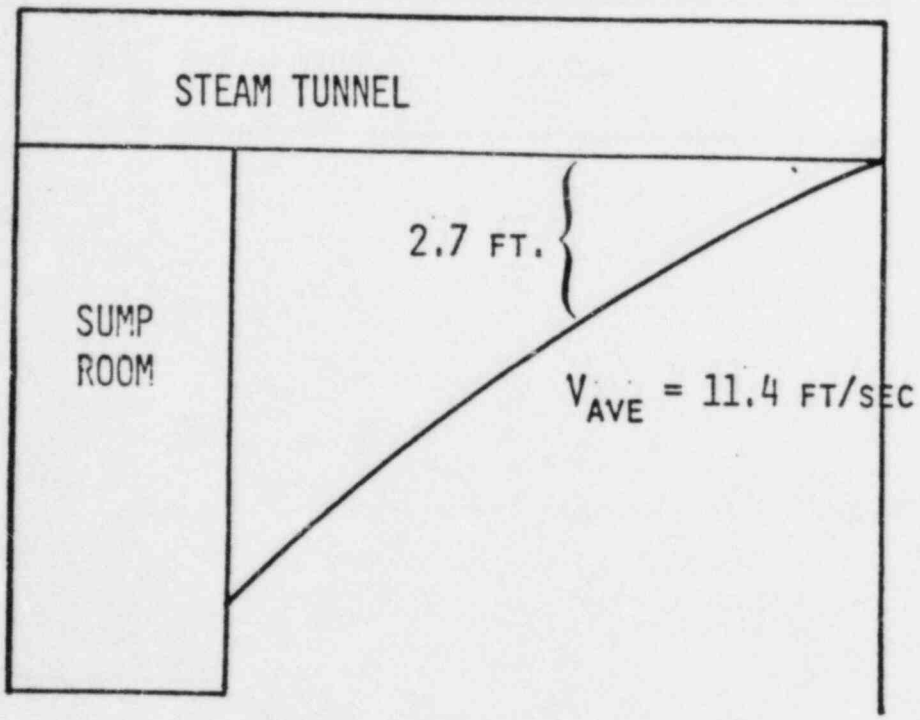

EJM
6/5/84

3. Combined effect of increased submergence and encroachments on local loads

The effects of increased sumbergence and encroachment have been separately addressed. Bubble collapse was modeled by energy analysis to yield a source strength. An acoustic model was then utilized for evaluation of wall loads caused by bubble collapse within the suppression pool. These same techniques are appropriate for the determination of the combined effects of submergence and encroachments.

The separate effects of submergence and encroachments were shown to be bounded by existing design load conservatisms. This was accomplished using single cell pool modeling of the acoustic chug response. For the combined effects of submergence and encroachments a multiple cell model was used to demonstrate that the GESSAR local chugging load is adequate. Thus, the pool acoustic model was modified to account for one source in each of three cells, as shown in Figure 1.

Reference 1 demonstrated that the GESSAR global chugging load definition bounds the load arising from the maximum chug placed at all vents, when desynchronized. The GESSAR global load definition uses the mean chug at all vents in synchrony. For this response, the three cell acoustic model was driven with a maximum chug source at the center cell and the mean chug data at the outer two cells. The loads were applied synchronously. This synchronous mean-max-mean chug model, while more realistic than the model used in the previous evaluation is still a conservative bound of the suppression pool chugging phenomena.

Acutual test data from General Electric's Pressure Suppression Test Facility (PSTF) was used as input into the modified acoustic model. The maximum chug pressure measured in the full scale PSTF chugging tests (Test 5707, Run 11, Chug 78) was increased by 10% to account for the additional 4.5 ft. submergence. This was used as the source for the center vent system. The outer vent systems used this same increased pressure but multiplied by 24% to obtain mean chug sources. The modified acoustic code was then run for an 11.9' encroachment. The maximum pressure at each location in the containment wall was averaged to obtain the area average peak pressure on the wall. A ratio of the pressures between this case and the previously performed base case, consisting of a single vent maximum chug pressure system, was found. This ratio was applied to the ARS of the maximum measured PSTF chug and then campared with the local load defintion ARS. This procedure was also performed in the drywell wall and basemat.

The three vent system with increased submergence and encroachment showed a 1% increase on the containment over the maximum test data chug. The basemat demonstrated a 7% decrease and the drywell wall showed no change in loading. Comparison plots between these loads and the GESSAR II local load definition are shown in Figures 2 through 4.

It is concluded that the combined effects of increased submergence and encroachment are easily bound by the existing load definition.

Reference

(1) GESSAR II, Appendix 3B, Section 3BO.3.2.16

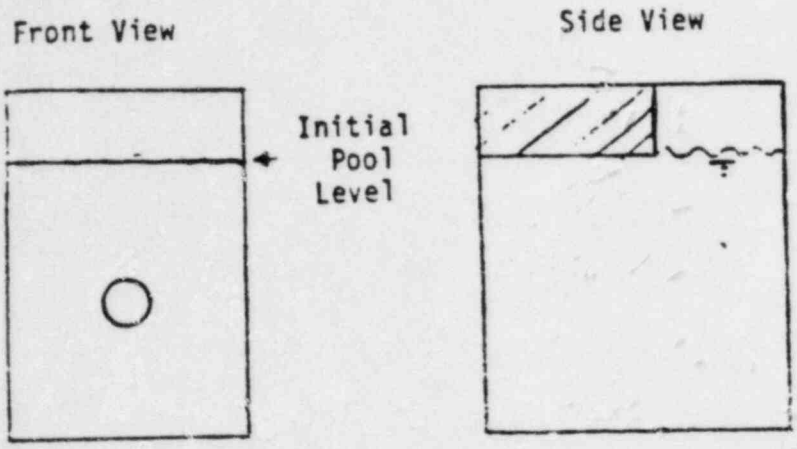

One Vent System

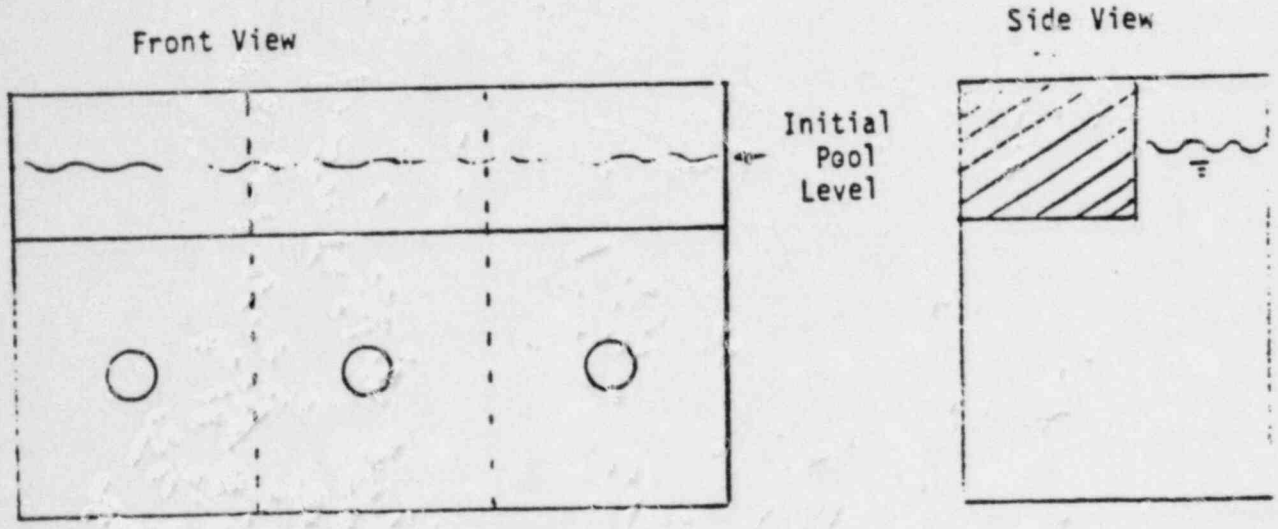

Three Vent System

Figure 1

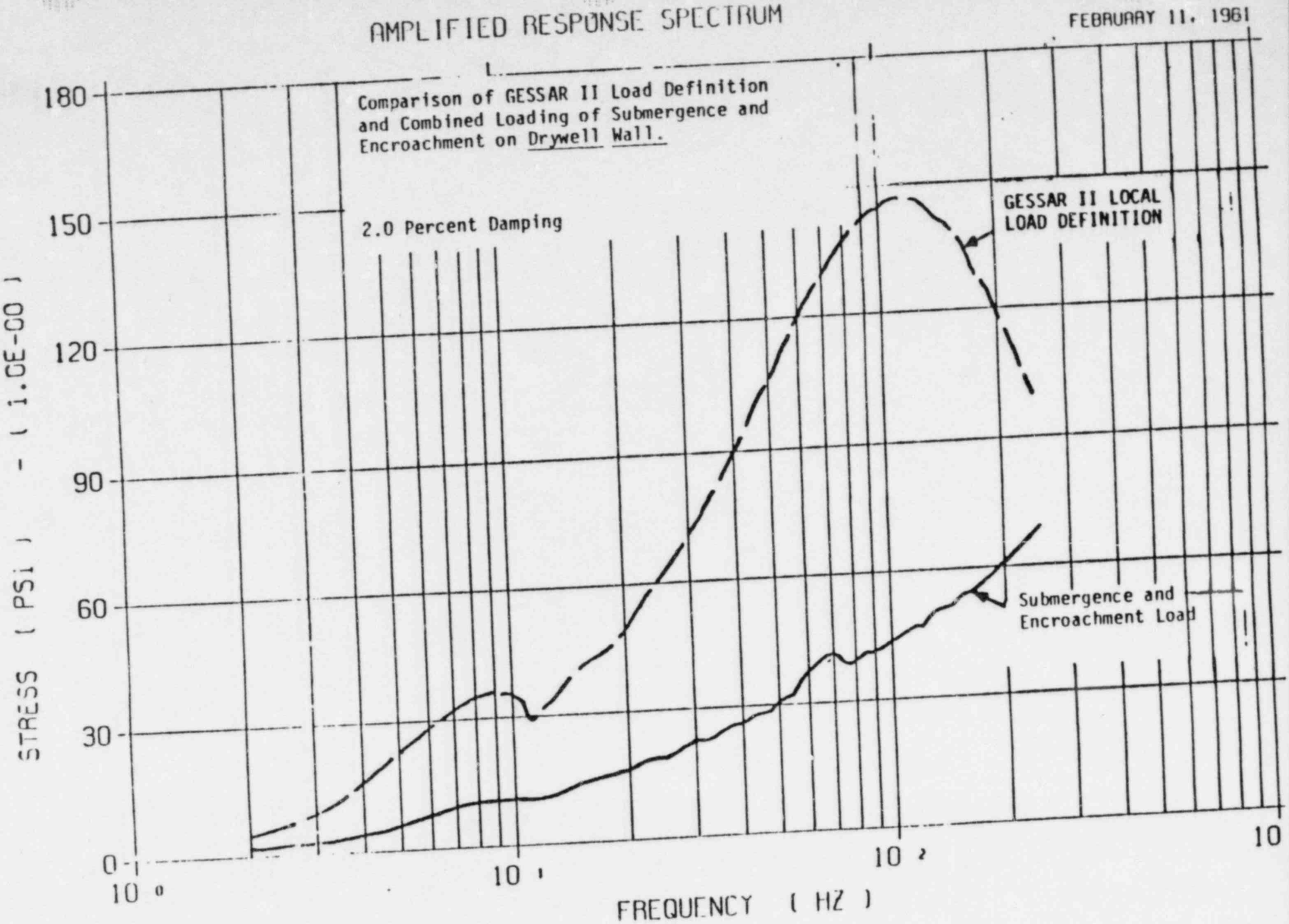
AMPLIFIED RESPONSE SPECTRUM
FEBRUARY 11, 1981
Comparison of GESSAR II Load Definition and Combined Loading of Submergence and Encroachment on Drywell Wall.
2.0 Percent Damping
GESSAR II LOCAL LOAD DEFINITION
Submergence and Encroachment Load
STRESS (PSi) - (1.0E-00)
180
150
120
90
60
30
0
10 0
10 1
10 2
10
FREQUENCY (HZ)

Figure 2

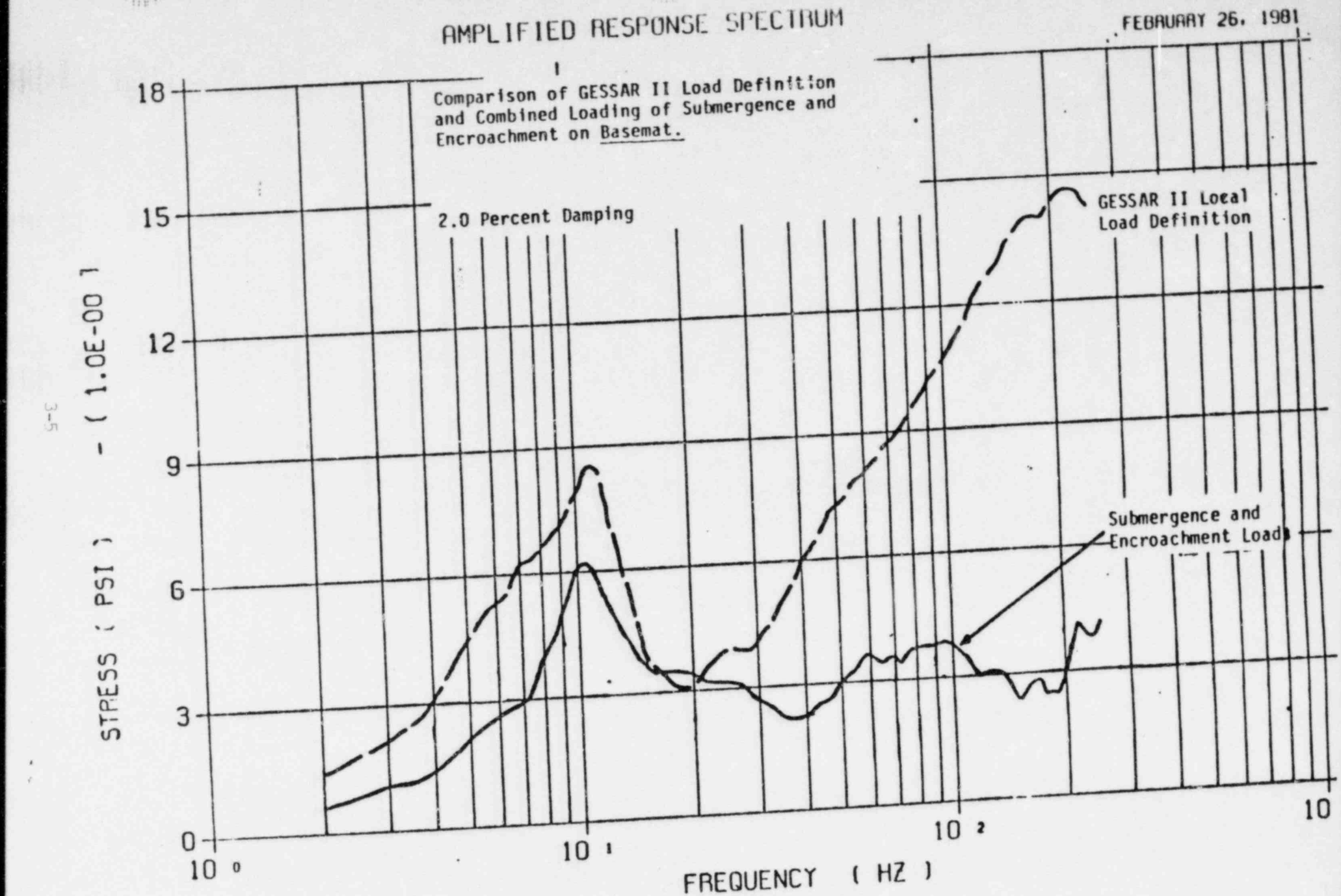
AMPLIFIED RESPONSE SPECTRUM
FEBRUARY 26, 1981
Comparison of GESSAR II Load Definition and Combined Loading of Submergence and Encroachment on Basemat.
2.0 Percent Damping
GESSAR II Local Load Definition
Submergence and Encroachment Load
STRESS (PSI) - (1.0E-00)
FREQUENCY (HZ)
18
15
12
9
6
3
0
10 0
10 1
10 2
10

Figure 3

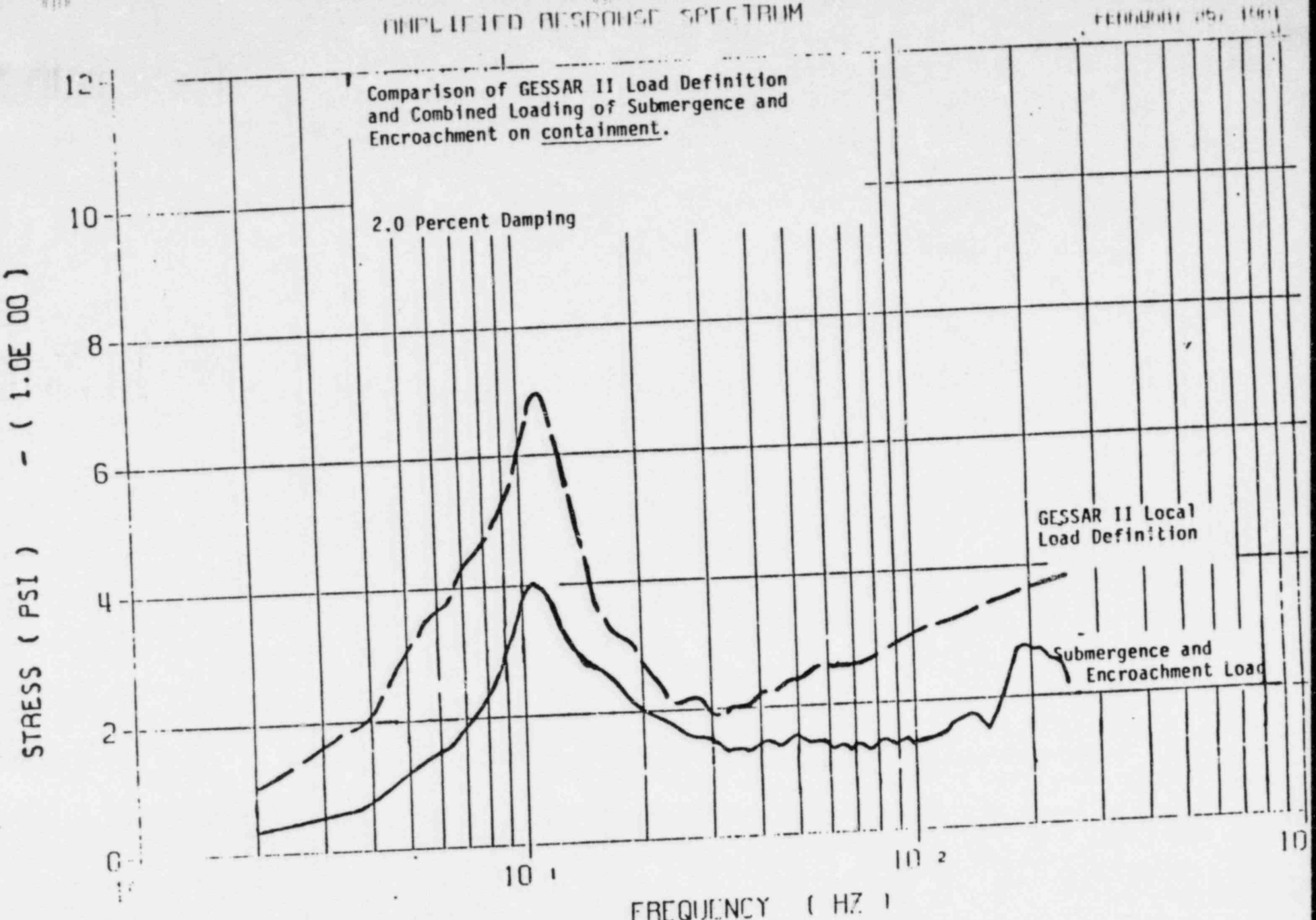
AMPLIFIED RESPONSE SPECTRUM
Comparison of GESSAR II Load Definition and Combined Loading of Submergence and Encroachment on containment.
2.0 Percent Damping
GESSAR II Local Load Definition
Submergence and Encroachment Load
STRESS (PSI) - (1.0E 00)
FREQUENCY (HZ)
0
2
4
6
8
10
12
10 1
10 2
10

Figure 4

4. Encroachments Effects on Main Steam SRV Loads".

Detailed analyses have been performed to determine the influence of the encroachment on 1) changes of the source phenomena, and 2) increases in pool boundary loads.

It was found that the only effect on source phenomena due to the encroachment was to lower the frequency of bubble oscillation by less than three percent. Conceptually, this is understood by realizing that the encroachment forces a larger volume of water to participate during bubble oscillation. This larger volume of water represents an increase in mass in an oscillatory system where all else remains unchanged. The three percent shift in frequency is bounded by the fifteen percent peak broadening, included as design margin, when applying the ARS of the load definition, and is therfore not of concern. In addition, the following source related occurences have been addressed and were found to be uninfluenced by the encroachment:

- SRV water clearing spike
- SRV discharge line maximum pressure
- SRV air clearing transient and subsequent coalescence into large air bubbles.
- SRV quencher condensation oscillation pressure amplitudes and frequency content.

An acoustic model of the suppression pool was used to determine increases in the normalized pool boundary loads due to SRV actuation. the input bubble pressure was a five hertz sine wave of unit amplitude. The acoustic model was qualified to predict SRV quencher attenuations using Caorso test data. Figures 1 and 2 show model-data comparisons on the containment and drywell wall respectively. To show that the Mark III plants will not experience adverse loadings from SRV discharge under their encroachment, a bounding Mark III case was executed Since a small pool and large encroachment are expected to maximize boundary loads, the bounding case modeled an 18.2' by 18.2' pool, partially covered by a 13' encroachment. These conditions are more severe than in any domestic Mark III plant. The resultant normalized wall pressure is compared to the 238 Standard Plant wall pressure in Figure 3. The only exceedences are on the drywell wall (which is bounded by the pool swell load difinition) and in the corner of the basemat and containment (which is small and a consequence of the severe conditions modelled which could not occur in any Mark III containment).

It is concluded that existing load definitions adequately bound all increases in SRV loads due to any pool encroachments.

Figure 1 Model - Data Comparison on Containment Wall

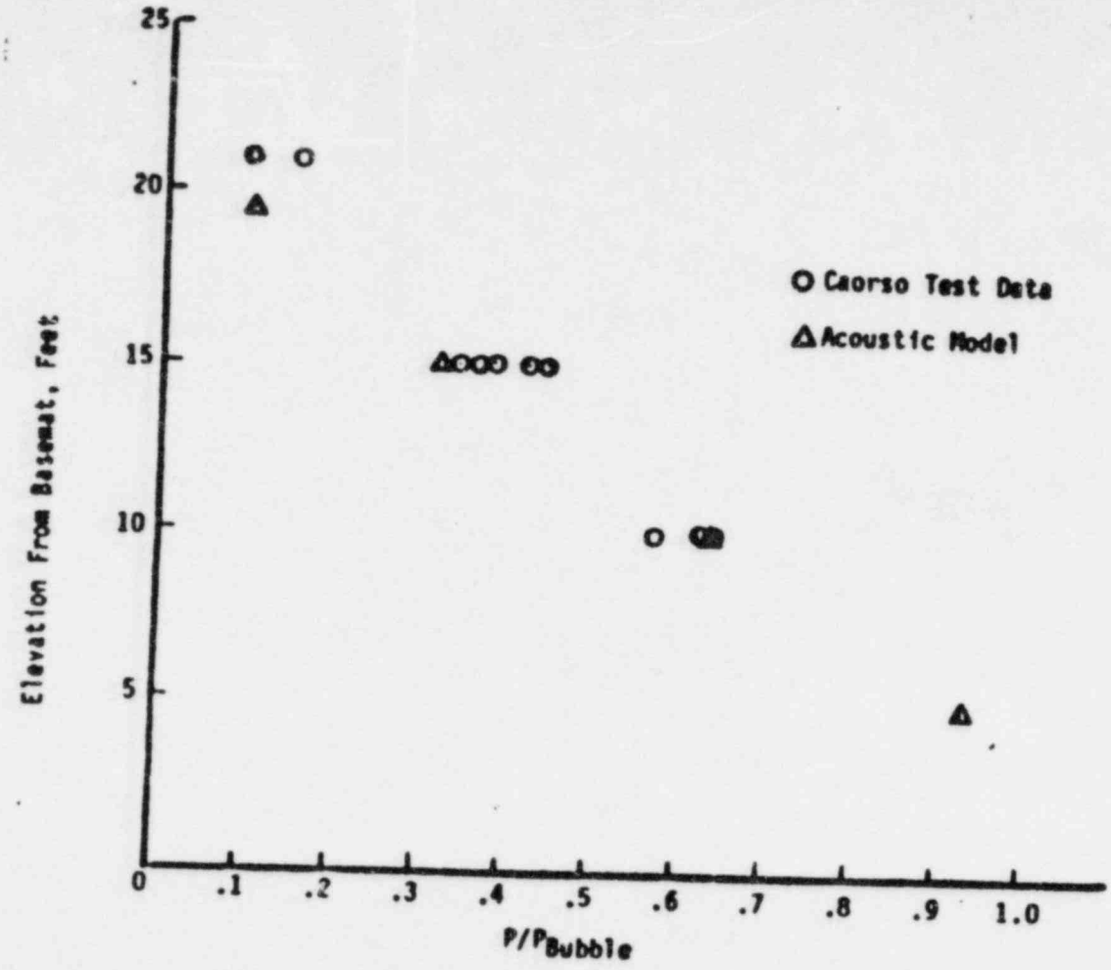

vlm - 3/83

Figure 2 Model - Data Comparison on Drywell Wall

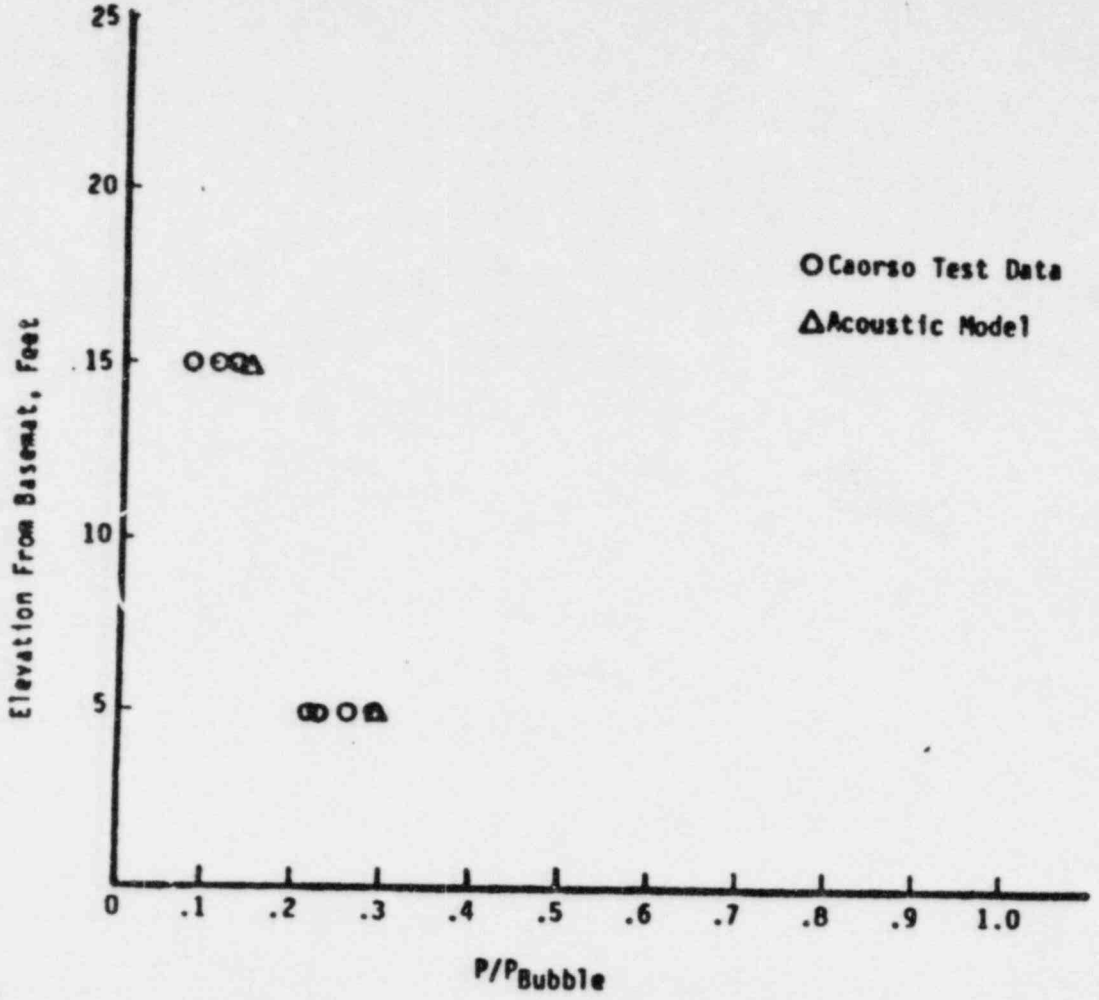

vlm - 3/83

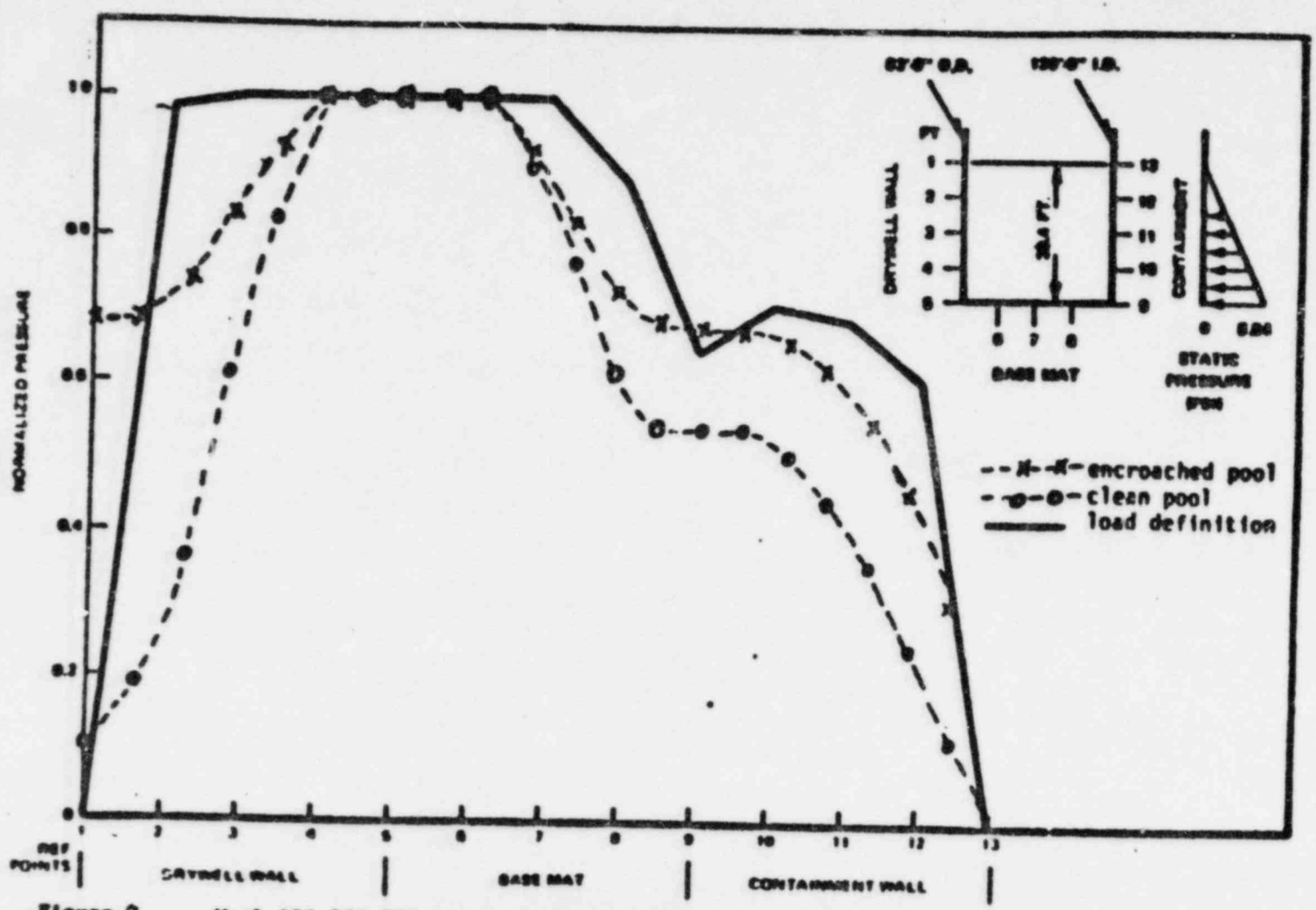

Figure 3 Mark III 238-732 Standard Plant One S/R Valve Normalized Wall Pressure at 4.5° compared with Bounding Mark III Encroachment Configuration Normalized Wall Pressure.